ELSEVIER

Journal of Organometallic Chemistry 525 (1996) 71–80

Journal of Organometallic Chemistry

# Synthesis, characterization and solution properties of organorhodium complexes derived from rhodoximes with one or two diphenylboron moieties in the oxime bridges

Fioretta Asaro [a], Renata Dreos [a,*], Silvano Geremia [b], Giorgio Nardin [a], Giorgio Pellizer [a], Lucio Randaccio [a], Giovanni Tauzher [a], Sara Vuano [a]

[a] *Dipartimento di Scienze Chimiche, Università di Trieste, 34127 Trieste, Italy*
[b] *Dipartimento di Scienze dei Materiali e della Terra, Università di Ancona, 60131 Ancona, Italy*

Received 20 February 1996

**Abstract**

The reaction between methylrhodoxime, $CH_3Rh(DH)_2L$ (L = N–MeIm or Py), and diphenylborinic anhydride affords derivatives containing either one or two diphenylboryl bridges, depending on the ratio complex:diphenylborinic anhydride. Kinetic studies show that the insertion of the diphenylboryl bridges is a two-step process involving the formation of a relatively stable intermediate. The X-ray structure of $CH_3Rh(DH)(DBPh_2)$N–MeIm shows that the axial phenyl faces the N–MeIm, whereas the main conformation in solution, as inferred from $^1H$ NMR spectra, has the axial phenyl facing the methyl. The bis(diphenylborylated) derivatives are less stable than those of the corresponding cobaloximes, and adopt a conformation with *trans* axial phenyls.

*Keywords:* Rhodium; Rhodoximes; Boron bridges; Kinetics; X-ray structures; NMR spectra

## 1. Introduction

Metal complexes with substituted bis(dimethylglyoximato) have received increasing attention in the last years. For instance, derivatives of cobaloximes with modified equatorial moieties have been synthesized in order to better mimic some specific properties of the Vit.$B_{12}$ coenzyme, such as reversible homolysis of the Co–C bond when it is bound to the apoenzyme [1], or in order to avoid undesired side reactions, such as autoxidation of the metal center when the Co(II) complexes are studied as oxygen carriers [2].

Modifications of the bis(dimethylglyoximato) ligand can also provide supramolecular properties for complexes. This can be achieved in a relatively simple way, replacing the hydrogen bonds with boron bridges by reaction with boron trifluoride or with derivatives of the diphenylborinic acid. The resulting Co and Ni derivatives have been known for a long time [3]; the analogous Fe(II) complexes have been synthesized and thoroughly investigated more recently [4]. The Fe(II) derivatives containing diphenylboryl bridges may assume various conformations in solution; the preferred conformation was inferred from $^1H$ NMR spectra, owing to the large upfield shift of the resonances of the ligands facing the axial phenyl [4]. The systematic examination of a large number of these complexes [4], with axial ligands spanning from good π-donors to good π-acceptors, showed that complexes having two identical axial ligands usually adopt a $C_{2h}$ conformation; when the axial ligands differ, the equatorial moiety may adopt either a $C_{2h}$ (Fig. 1(a)) or a $C_{2v}$ (Fig. 1(b)) conformation, in order to energetically optimise the non-bonding π–π interactions; the attractive CH–π interactions play a minor role [4]. In most of the bis(dimethyglyoximato) derivatives examined so far, both the hydrogen bonds were replaced and the resulting macrocycle was very stable in solution. Recently, we reported that $CH_3Co(DH)_2L$ (L = N–MeIm or Py) is able to give both mono- and bis(diphenylborylated) complexes, depending on the ratio complex:diphenylborinic anhydride [5], both of these derivatives being quite stable in solution. The X-ray crystal structures showed that in $CH_3Co(DH)(DBPh_2)$N–MeIm the axial phenyl faces

* Corresponding author.


*PII* S0022-328X(96)06479-0

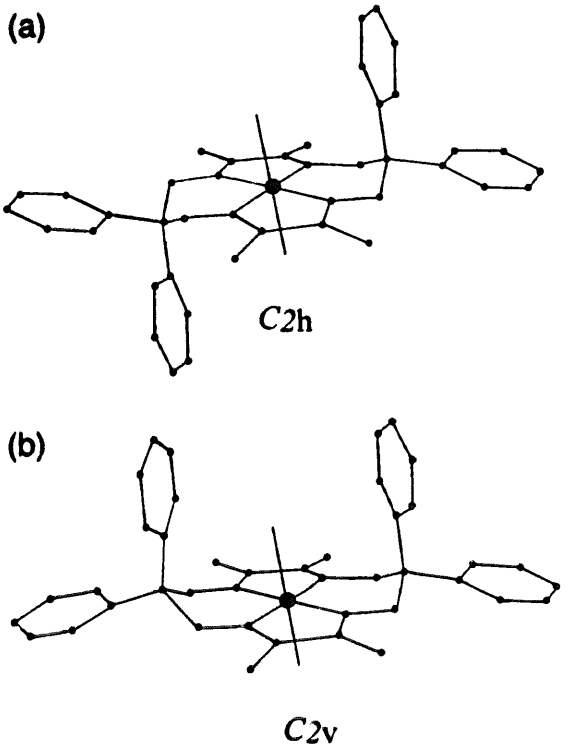


Fig. 1. Possible conformations of the equatorial ligand: (a) $C_{2h}$; (b) $C_{2v}$.

the methyl and that $CH_3Co(DBPh_2)_2CH_3OH$ adopts a $C_{2h}$ conformation. The conformations in solution, as inferred from $^1H$ NMR spectra, agree with these results [5].

Attempts to perform a kinetic study of the insertion of boryl bridges in methylcobaloximes were unsuccessful, because the reactions are so slow that parallel decomposition of the Co–C occurs [6]. It is well known that the Rh–C bond is more stable than the Co–C bond towards homolysis [7], whereas several other structural and reactivity properties of the organorhodoximes parallel those of the corresponding organocobaloximes [8–10]. Therefore we decided to extend our studies to methylrhodoximes; this comparison could also furnish an insight into the role of the metal center in determining the stability and conformations adopted both in solution and in solid state by the borylated complexes. We report here results concerning the synthesis and characterization of some $CH_3Rh(DH)(DBPh_2)L$ and $CH_3Rh(DBPh_2)_2L$ derivatives; solution studies of the insertion of the boron bridges allow the stability of the monoborylated derivatives to be rationalized and related to the structure in the solid state.

## 2. Experimental

### 2.1. Materials and methods

Diphenylborinic anhydride and solvents were purchased and used without further purification.

$CH_3Rh(DH)_2N$–MeIm, $CH_3Rh(DH)_2Py$, and $CH_3Rh(DH)_2H_2O$ were prepared as reported previously [11]. In order to obtain X-ray quality crystals, $CH_3Rh(DH)_2N$–MeIm (**I**) was recrystallized from methanol with a slight excess of N–MeIm to prevent the dissociation of the axial base.

### 2.2. Physical measurements

Visible spectra and kinetics were recorded on a Uvikon 941 Plus spectrophotometer. $^1H$ and $^{13}C$ spectra were recorded on a Jeol EX-400 ($^1H$ at 400 MHz and $^{13}C$ at 100.4 MHz) from $CDCl_3$ solutions and using TMS as internal standard.

### 2.3. Syntheses

#### 2.3.1. $CH_3Rh(DH)(DBPh_2)N$–MeIm (II) and $CH_3Rh(DH)(DBPh_2)Py$ (III)

0.1 g of $CH_3Rh(DH)_2N$–MeIm (0.2 mmol) or respectively $CH_3Rh(DH)_2Py$ (0.2 mmol) and 0.04 g of $(BPh_2)_2O$ (0.1 mmol) were dissolved in $CH_2Cl_2$ at room temperature and allowed to react for 2 h. The partial removal of the solvent and the addition of isopropyl alcohol gave a yellow product, which was filtered and dried in vacuo.

**II**. Anal. Found: C, 49.7; H, 5.4; N, 13.2. $C_{25}H_{32}N_6O_4BRh$ Calc.: C, 50.5; H, 5.4; N, 14.1%.

**III**. Anal. Found: C, 51.3; H, 5.2; N, 12.2. $C_{26}H_{31}N_5O_4BRh$ Calc.: C, 52.8; H, 5.3; N, 11.8 N%.

X-ray quality crystals of **II** were obtained by recrystallization from $CH_2Cl_2/CH_3OH$ in the presence of a slight excess of N–MeIm.

#### 2.3.2. $CH_3Rh(DBPh_2)_2N$–MeIm (IV)

This compound was prepared similarly, but a fourfold excess of diphenylborinic anhydride was added and the mixture was refluxed at 40 °C for one day. Removal of the solvent afforded a yellow powder, which was filtered and dried in vacuo. Anal. Found: C, 57.2; H, 5.5; N, 10.4. $C_{37}H_{41}N_6O_4B_2Rh$ Calc.: C, 58.7; H, 5.3; N, 11.1%. Attempts to recrystallize **IV** from $CH_2Cl_2/CH_3OH$ in the presence of a slight excess of N–MeIm afforded almost pure **II**.

#### 2.3.3. $CH_3Rh(DBPh_2)_2H_2O$ (V)

$CH_3Rh(DH)_2H_2O$ (0.1 g, 0.3 mmol) was dissolved in $CH_2Cl_2$/acetone and a few drops of water were added. After addition of 0.4 g (1.1 mmol) of diphenylborinic anhydride, the solution was refluxed at 40 °C for two days. Evaporation of the solvent afforded a yellow precipitate. Anal. Found: C, 56.8; H, 5.3; N, 8.2. $C_{33}H_{37}N_4O_5B_2Rh$ Calc.: C, 57.1; H, 5.4; N, 8.1%.

### 2.4. Kinetic studies

The kinetics were followed spectrophotometrically in $CH_2Cl_2$ at 25 °C. The initial concentration of **I** was in

the range $1.5–3.0 \times 10^{-4}$ M and a ten-fold excess of N–MeIm was added to prevent the dissociation of the axial base. The concentration of free anhydride, $[An]_f$, was calculated accounting for the equilibrium relative to the formation of a donor–acceptor complex between anhydride and N–MeIm (see below) and ranged from $4.2 \times 10^{-4}$ M to $3.5 \times 10^{-3}$ M for the first step and from $1.1 \times 10^{-3}$ M to $1.8 \times 10^{-2}$ M for the second step.

### 2.5. Determination of the formation constant of N–MeIm.$(BPh_2)_2O$

It is well known that the tricoordinate derivatives of boron form complexes with donor molecules [12]. The equilibrium constant relative to the association reaction

$$(BPh_2)_2O + \text{N–MeIm} \rightleftharpoons \text{N–MeIm}.(BPh_2)_2O$$

in $CH_2Cl_2$ at 25.5 °C was determined by spectrophotometric titrations at 244 nm. With the use of a microsyringe, a $3 \times 10^{-1}$ M solution of N–MeIm was added stepwise to a $5 \times 10^{-5}$ M solution of diphenylborinic anhydride, so that the volume of the solution was increased by no more than 2%. Since the absorbance of N–MeIm is not negligible at high concentration, the $A_\infty$ value, i.e. the absorbance of the complex, was extrapolated from the plot

$$A = A_\infty - (A - A_0)/K[\text{N–MeIm}]$$

where $A$ is the measured absorbance and $A_0$ is the absorbance of the diphenylborinic anhydride solution. The $K$ value ($3.7 \pm 0.5 \times 10^3$ $M^{-1}$) was obtained as the intercept of the plot

$$\log[(A - A_0)/(A_\infty - A)] = \log K + \log[\text{N–MeIm}]$$

The slope ($0.99 \pm 0.01$) close to 1 confirms the 1:1 stoichiometry of the complex between anhydride and N–MeIm under these experimental conditions.

### 2.6. Crystallographic studies

Crystals of complexes **I** and **II**, suitable for X-ray structure determination, were obtained according to the procedures reported above. Preliminary examination and data collection were performed with Mo Kα radiation ($\lambda = 0.70930$ Å) on an Enraf–Nonius CAD4 single-crystal diffractometer equipped with a graphite-monochromator. Reflections with $I \geq 3\sigma(I)$ were corrected for Lorentz and polarization effects. Empirical absorption corrections based on Ψ-scan data were applied to the reflection intensities only for **I**. No absorption correction was applied for **II**, owing to the small size of the crystal used. Isotropic extinction correction was applied to the data and the coefficient of the secondary extinction [13] was refined in the final least-square cycles. Crystal data and some details of data collection are summarized in Table 1.

The structures were solved by conventional Patterson and Fourier methods. H atoms, at calculated geometrical positions, were located on the difference Fourier map. Final full-matrix anisotropic least-squares refinements,

Table 1
Crystallographic data

| Compound | I | II |
|---|---|---|
| Formula | $RhO_4N_6C_{11}H_{24}$ | $RhO_4N_6C_{23}BH_{32}$ |
| $M$ | 430.27 | 594.29 |
| $a$ (Å) | 9.278(1) | 11.087(1) |
| $b$ (Å) | 11.749(1) | 20.593(3) |
| $c$ (Å) | 16.583(3) | 23.577(5) |
| $\beta$ (deg) | 96.580(7) | |
| $V$ (Å$^3$) | 1795.8(4) | 5383(2) |
| $Z$ | 4 | 8 |
| Space group | $P2_1/n$ | $Pbca$ |
| $D_{calc}$ (g cm$^{-3}$) | 1.592 | 1.467 |
| $\mu$(Mo K) (cm$^{-1}$) | 9.6 | 6.6 |
| $F$(000) | 880 | 2448 |
| Crystal size (mm$^3$) | 0.7x0.4x0.6 | 0.2x0.3x0.3 |
| Transmission max. min (%) | 79.6–99.6 | |
| $2\theta$(Mo K) (deg) | 60 | 60 |
| Second extinction | $5.23(3) \times 10^{-7}$ | $2.8(5) \times 10^{-8}$ |
| No. measured reflections | 5623 | 7778 |
| No. independent reflections [$I \geq 3\sigma(I)$] | 4073 | 3575 |
| No. variables | 218 | 335 |
| Weight | 1 | $4F^2/[\sigma(I) + (0.04F)^2]$ |
| $R(F_o)$ | 0.024 | 0.039 |
| $R_w(F_o)$ | 0.025 | 0.044 |
| Goodness of fit | 0.89 | 1.17 |
| Residuals in F-map (e Å$^{-3}$) | 0.36 | 0.61 |

Table 2
Positional parameters and $B_{eq}$ [a] (Å$^2$) for non-H atoms. The standard uncertainty is reported in parentheses

| Atom | x | y | z | $B_{eq}$ (Å$^2$) | x | y | z | $B_{eq}$ (Å$^2$) |
|---|---|---|---|---|---|---|---|---|
| | I | | | | II | | | |
| Rh | 0.03547(2) | 0.21284(1) | 0.34579(1) | 2.311(2) | 0.21636(3) | 0.12434(2) | 0.04333(1) | 2.624(5) |
| O1 | 0.1969(2) | 0.0067(2) | 0.3255(1) | 4.18(4) | −0.0128(3) | 0.1750(2) | 0.0090(2) | 4.48(8) |
| O2 | −0.2748(2) | 0.2294(2) | 0.3524(1) | 4.62(4) | 0.2597(3) | 0.0330(2) | 0.1350(2) | 3.41(7) |
| O3 | −0.1268(2) | 0.4176(2) | 0.3706(1) | 5.34(5) | 0.4440(3) | 0.0601(2) | 0.0727(1) | 3.53(7) |
| O4 | 0.3507(2) | 0.1992(2) | 0.3482(1) | 5.00(5) | 0.1797(4) | 0.2060(2) | −0.0579(2) | 4.93(9) |
| N1 | 0.0648(2) | 0.0479(2) | 0.3314(1) | 2.95(4) | 0.0411(3) | 0.1390(2) | 0.0468(2) | 3.41(8) |
| N2 | −0.1638(2) | 0.1568(2) | 0.3438(1) | 3.13(4) | 0.1769(3) | 0.0731(2) | 0.1099(2) | 2.93(8) |
| N3 | 0.0058(3) | 0.3774(2) | 0.3659(1) | 3.69(4) | 0.3902(3) | 0.1037(2) | 0.0375(2) | 3.00(7) |
| N4 | 0.2370(2) | 0.2701(2) | 0.3546(1) | 3.30(4) | 0.2609(4) | 0.1704(2) | −0.0273(2) | 3.48(9) |
| N5 | 0.0088(2) | 0.2336(2) | 0.2142(1) | 2.62(3) | 0.2413(3) | 0.2141(2) | 0.0903(2) | 2.92(8) |
| N6 | 0.0488(2) | 0.2870(2) | 0.0918(1) | 3.51(4) | 0.2981(4) | 0.3127(2) | 0.1130(2) | 3.55(8) |
| C1 | −0.0480(4) | −0.1416(3) | 0.3176(2) | 5.36(7) | −0.1493(5) | 0.1135(3) | 0.0944(3) | 5.0(1) |
| C2 | −0.0511(3) | −0.0156(2) | 0.3274(1) | 3.54(5) | −0.0155(4) | 0.1093(2) | 0.0883(2) | 3.4(1) |
| C3 | −0.1840(3) | 0.0488(2) | 0.3352(1) | 3.58(5) | 0.0641(4) | 0.0700(2) | 0.1243(2) | 3.3(1) |
| C4 | −0.3306(3) | −0.0050(3) | 0.3327(2) | 5.83(7) | 0.0188(5) | 0.0296(3) | 0.1723(3) | 5.2(1) |
| C5 | 0.1174(6) | 0.5658(3) | 0.3903(3) | 8.5(1) | 0.5751(5) | 0.1086(3) | −0.0196(3) | 5.3(1) |
| C6 | 0.1227(4) | 0.4402(2) | 0.3744(2) | 4.61(6) | 0.4471(4) | 0.1251(3) | −0.0068(2) | 3.36(9) |
| C7 | 0.2562(3) | 0.3778(2) | 0.3683(2) | 4.15(5) | 0.3715(5) | 0.1663(2) | −0.0442(2) | 3.8(1) |
| C8 | 0.4024(4) | 0.4332(3) | 0.3778(2) | 6.72(7) | 0.4208(6) | 0.1992(3) | −0.0948(3) | 5.4(1) |
| C9 | 0.0615(3) | 0.1864(2) | 0.4694(2) | 3.88(5) | 0.1839(5) | 0.0424(3) | −0.0045(2) | 4.1(1) |
| C10 | 0.0925(3) | 0.2945(2) | 0.1717(1) | 3.04(4) | 0.4672(5) | −0.0044(3) | 0.1606(2) | 3.7(1) |
| C11 | −0.0695(3) | 0.2179(3) | 0.0829(1) | 3.78(5) | 0.4181(5) | −0.0459(3) | 0.2014(2) | 3.9(1) |
| C12 | −0.0940(3) | 0.1855(2) | 0.1584(2) | 3.29(5) | 0.4856(6) | −0.0921(3) | 0.2293(3) | 5.2(1) |
| C13 | 0.1158(4) | 0.3434(4) | 0.0271(2) | 6.13(8) | 0.6064(6) | −0.0987(3) | 0.2167(3) | 5.6(1) |
| C14 | | | | | 0.6578(6) | −0.0587(4) | 0.1771(3) | 6.5(2) |
| C15 | | | | | 0.5892(5) | −0.0131(3) | 0.1491(3) | 5.4(1) |
| C16 | | | | | 0.4147(5) | 0.1200(3) | 0.1685(2) | 3.7(1) |
| C17 | | | | | 0.5057(6) | 0.1634(3) | 0.1554(3) | 5.6(2) |
| C18 | | | | | 0.5329(7) | 0.2161(4) | 0.1893(4) | 7.6(2) |
| C19 | | | | | 0.4691(7) | 0.2259(3) | 0.2384(3) | 7.9(2) |
| C20 | | | | | 0.3805(8) | 0.1837(3) | 0.2536(3) | 6.9(2) |
| C21 | | | | | 0.3524(6) | 0.1310(3) | 0.2190(2) | 5.4(1) |
| C22 | | | | | 0.1911(5) | 0.2307(2) | 0.1410(2) | 3.5(1) |
| C23 | | | | | 0.2256(6) | 0.2911(3) | 0.1553(2) | 4.1(1) |
| C24 | | | | | 0.3048(4) | 0.2650(2) | 0.0745(2) | 3.3(1) |
| C25 | | | | | 0.3583(6) | 0.3746(3) | 0.1100(3) | 5.4(1) |
| B | | | | | 0.3925(5) | 0.0548(3) | 0.1326(3) | 3.3(1) |

[a] Anisotropically refined atoms are given in the form of the isotropic equivalent displacement parameter defined as $(4/3)[a^2B(1,1) + b^2B(2,2) + c^2B(3,3) + ab(\cos\gamma)B(1,2) + ac(\cos\beta)B(1,3) + bc(\cos\alpha)B(2,3)]$.

with the fixed contribution of hydrogen atoms ($B = 1.3B_{eq}$ of the atom to which they are attached) converged to the $R$ and $R_w$ values reported in Table 1. Final non-hydrogen positional parameters and $B_{eq}$ values are given in Table 2. Atomic scattering factors, anomalous dispersion terms and programs were taken from the Enraf–Nonius MolEN package [14]; see also supplementary material.

## 3. Results

### 3.1. Syntheses

All the products were obtained by reaction of the parent methylrhodoxime with diphenylborinic anhydride.

The monoborylated complexes **II** and **III** were obtained by reacting the corresponding rhodoximes with less than stoichiometric anhydride, and were characterized by both elemental analysis and NMR spectra. **II** was also characterized by X-ray crystal structure determination. **IV** was isolated in the presence of an excess of diphenylborinic anhydride, and the elemental analysis is quite satisfactory if allowance is made for the presence of traces of solvent. No X-ray quality crystals could be obtained, because attempts at recrystallization led to loss of one boryl bridge and to formation of **II**. Indeed, $^1$H NMR spectra showed that a mixture of **II**, **IV**, and **V** was immediately formed on dissolving **IV** in $CDCl_3$. **V** comes from the substitution of the axial base by the water present as traces in $CDCl_3$, and its formation may be prevented by adding a slight excess of N–MeIm.

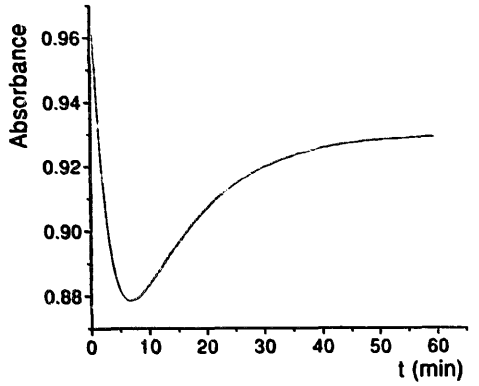


Fig. 2. Variation in absorbance at 310 nm on addition of diphenylborinic anhydride to $CH_3Rh(DH)_2N$–MeIm. $[CH_3Rh(DH)_2N\text{–MeIm}]_0 = 1.5\times10^{-4}$ M, $[N\text{–MeIm}]_0 = 1.5\times10^{-3}$ M, $[An]_f = 2.6\times10^{-3}$ M; solvent $CH_2Cl_2$, $T = 25$°C.

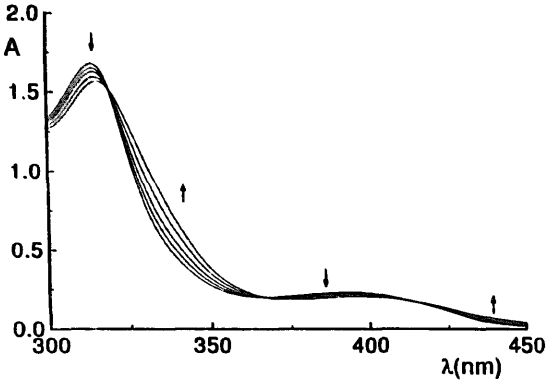


Fig. 3. Spectral changes due to the insertion of the first diphenylboryl bridge in $CH_3Rh(DH)_2N$–MeIm. $[CH_3Rh(DH)_2N\text{–MeIm}]_0 = 1.7\times10^{-4}$ M, $[N\text{–MeIm}]_0 = 1.7\times10^{-3}$ M, $[An]_f = 2.7\times10^{-4}$ M; solvent $CH_2Cl_2$, $T = 25$°C.

Stepwise additions of diphenylborinic anhydride to $CH_3Rh(DH)_2L$ (L = N–MeIm, Py, or $PPh_3$) in $CDCl_3$, followed by $^1H$ NMR spectroscopy, showed that the monoborylated species was prevalent for complex:anhydride ratios less than 1:1. A two-fold excess of the borylated agent led to the complete formation of $CH_3Rh(DBPh_2)_2L$ for L = Py or N–MeIm, but a four-fold excess was necessary when the axial base was $PPh_3$.

As for the analogous Co complexes [5], the monoborylated derivative of the aqua-complex was never detected. Indeed, the $^1H$ NMR spectra of the solutions prepared by mixing equimolar amounts of $CH_3Rh(DH)2H_2O$ and anhydride in $CDCl_3$ showed a mixture of the starting rhodoxime, the final product **V** and a not well-characterized organometallic species **VI** containing one boron bridge [1]. At higher anhydride:complex ratios, only **V** and **VI** were present in solution in an approximately constant relative amount.

### 3.2. Kinetic results

The formation of **IV** starting from **I** and diphenylborinic anhydride involves two consecutive steps (Fig. 2). The reaction rates are not very different, but the reactions can be studied separately by an appropriate choice of the wavelength. Indeed, both spectra pertinent to the insertion of the first boron bridge (Fig. 3), which is the only process evident at free anhydride:complex ratios of about one, and spectra pertinent to the insertion of the second boron bridge (Fig. 4), monitored at higher free anhydride:complex ratios, show well-developed isosbestic points. Therefore, the first reaction was studied at $\lambda$ ranging between 435 and 447 nm, where the change of absorbance due to the second reaction is close to zero and the second reaction was followed at 413 nm, the isosbestic point for the first reaction. In order to minimize the overlap of the two stages, the first points of the kinetics of the second reaction were discarded. The kinetics were carried out under pseudo-first-order conditions, i.e. in the presence of an excess of diphenylborinic anhydride. The plots of $\log(A_t - A_\infty)$, where $A_t$ is the absorbance at time $t$ and $A_\infty$ is the final absorbance, versus time were linear and allowed the calculation of $k_{1obs}$ and $k_{2obs}$.

The plots of $k_{obs}$ vs. $[An]_f$ were linear

$$k_{1obs} = k_1[An]_f \quad \text{I step}$$

$$k_{2obs} = k_2[An]_f \quad \text{II step}$$

and did not show an intercept, revealing that under these experimental conditions the reactions go to completion (Figs. 5 and 6).

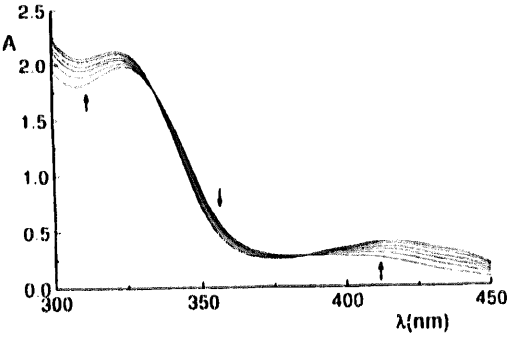


Fig. 4. Spectral changes due to the insertion of the second diphenylboryl bridge in $CH_3Rh(DH)_2N$–MeIm. $[CH_3Rh(DH)_2N\text{–MeIm}]_0 = 3\times10^{-4}$ M, $[N\text{–MeIm}]_0 = 3\times10^{-3}$ M, $[An]_f = 7.1\times10^{-3}$ M; solvent $CH_2Cl_2$, $T = 25$°C.

[1] $^1H$ NMR spectra show that the species **VI** contains an axial methyl ($\delta$ 0.4 ppm), a monoborylated equatorial moiety ($\delta$ 2.28 and 2.42 ppm), and probably a molecule of anhydride or diphenylborinic acid arising from its hydrolysis as a *trans* axial ligand. Addition of water to a solution of **V** and **VI** decreased the concentration of the latter, increasing that of the aqua-derivative and therefore supporting the hypothesis of a different axial coordination for **VI**.

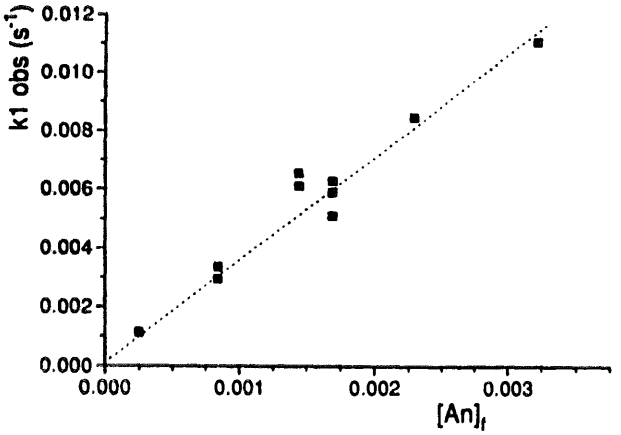


Fig. 5. Dependence of $k_{1obs}$ on free anhydride concentration for the insertion of the first diphenylboryl bridge in $CH_3Rh(DH)_2N$–MeIm. Solvent $CH_2Cl_2$, $T = 25°C$.

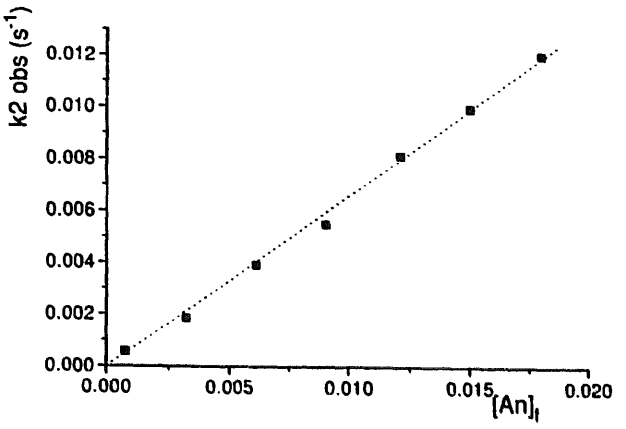


Fig. 6. Dependence of $k_{2obs}$ on free anhydride concentration for the insertion of the second diphenylboryl bridge in $CH_3Rh(DH)_2N$–MeIm. Solvent $CH_2Cl_2$, $T = 25°C$.

Both $k_1$ ($3.32\,M^{-1}\,s^{-1}$) and $k_2$ ($0.67\,M^{-1}\,s^{-1}$) are independent of the concentration of free N–MeIm (i.e. accounting for the association with anhydride, see Section 2).

The ratio $k_1/k_2 \approx 5$ indicates the formation of a relatively stable intermediate, in accordance with the findings of NMR titration and with the possibility of isolating the $CH_3Rh(DH)(DBPh_2)N$–MeIm complex in defect of anhydride.

### 3.3. NMR spectra

The $^{13}C$ NMR data are reported in Table 3. The spectra of **II** and **III** show two well distinct signals, both for the equatorial CN and for the equatorial $CH_3$,

Table 3
$^{13}C$ NMR data for $CH_3Rh(DH)_{2-n}(DBPh_2)_nL$

*$CH_3Rh(DH)_{2-n}(DBPh_2)_nH_2O$*

| | $DBPh_2$ | | | | | DH | | $CH_3ax$ [b] |
|---|---|---|---|---|---|---|---|---|
| | *ortho* | *meta* | *para* | CN | $CH_3$ | CN | $CH_3$ | |
| $n = 0$ | | | | | | 152.3 | 12.6 | 12.1 (22) |
| $n = 2$ | 131.8<br>131.6 | 128.0<br>127.2 | 126.4<br>126.3 | 154.9 | 13.2 | | | 4.75 (24) |

*$CH_3Rh(DH)_{2-n}(DBPh_2)_nPy$*

| | $DBPh_2$ | | | | | DH | | $CH_3ax$ [b] | Py | | |
|---|---|---|---|---|---|---|---|---|---|---|---|
| | *ortho* | *meta* | *para* | CN | $CH_3$ | CN | $CH_3$ | | *ortho* | *meta* | *para* |
| $n = 0$ | | | | | | 149.5 | 11.8 | −0.6 (23) | 149.6 | 125.7 | 137.8 |
| $n = 1$ | 131.9<br>131.8 | 127.2<br>127.1 | 126.0<br>125.4 | 154.4 | 13.0 | 148.9 | 12.0 | 3.4 (22) | 149.0 | 125.4 | 137.5 |
| $n = 2$ | 132.1<br>132.0 | 127.1<br>126.9 | 126.0<br>125.8 | 153.7 | 13.1 | | | 6.9 (22) | 146.8 | 124.7 | 136.6 |

*$CH_3Rh(DH)_{2-n}(DBPh_2)_nN$–MeIm*

| | $DBPh_2$ | | | | | DH | | $CH_3ax$ [b] | N–MeIm | | | |
|---|---|---|---|---|---|---|---|---|---|---|---|---|
| | *ortho* | *meta* | *para* | CN | $CH_3$ | CN | $CH_3$ | | C-2 | C-4 | C-5 | $CH_3$ |
| $n = 0$ | | | | | | 148.6 | 11.8 | −0.35 (22) | 137.1 | 128.0 | 121.1 | 34.1 |
| $n = 1$ | 132.2<br>132.1 | 127.1<br>127.0 | 125.5<br>125.4 | 153.7 | 12.9 | 148.2 | 11.9 | 3.2 (22) | 137.2 | 127.4 | 120.7 | 34.3 |
| $n = 2$ | 132.2<br>132.2 | 127.0<br>126.8 | 125.8<br>125.6 | 153.1 | 12.9 | | | 7 | 136.9 | 126.2 | 119.8 | 34.3 |

[a] δ Values (ppm from TMS) from $CDCl_3$ solutions at room temperature.
[b] $^1J$[Rh,C] (Hz) in parentheses.

Table 4
$^1$H NMR data for $CH_3Rh(DH)_{2-n}(BPh_2)_nL$ [a]

| | DBPh$_2$ | | | | DH | CH$_3$ax [b] | | | | |
|---|---|---|---|---|---|---|---|---|---|---|
| *$CH_3Rh(DH)_{2-n}(BPh_2)_nH_2O$* | *ortho* | *meta* | *para* | CH$_3$ | CH$_3$ | | | | | |
| $n=0$ | | | | | 2.22 | 0.71 (2.4) | | | | |
| $n=2$ | 7.51 | 7.23 | 7.20–7.15 | 2.50 | | 0.4 | | | | |
| | 7.20–7.15 | 7.11 | 7.01 | | | (2.4) | | | | |
| *$CH_3Rh(DH)_{2-n}(BPh_2)_nPy$* | DBPh$_2$ | | | | DH | CH$_3$ax [b] | Py | | | |
| | *ortho* | *meta* | *para* | CH$_3$ | CH$_3$ | | *ortho* | *meta* | *para* | |
| $n=0$ | | | | | 2.15 | 0.28 (2.4) | 8.49 | 7.32 | 7.73 | |
| $n=1$ | 7.57 | 7.18 | 7.08 | 2.42 | 2.20 | −0.33 | 8.39 | 7.26 | 7.68 | |
| | 7.31 | 7.18 | 7.08 | | | (2) | | | | |
| $n=2$ | 7.33 | 7.19 | 7.13 | 2.50 | | −0.18 | obs | 7.02 | obs | |
| | obs | 6.84 | 6.84 | | | (2) | | | | |
| *$CH_3Rh(DH)_{2-n}(BPh_2)_nN$-Melm* | DBPh$_2$ | | | | DH | CH$_3$ax [b] | N-MeIm | | | |
| | *ortho* | *meta* | *para* | CH$_3$ | CH$_3$ | | H-2 | H-4 | H-5 | CH$_3$ |
| $n=0$ | | | | | 2.14 | 0.16 (2) | 7.32 | 6.82 | 6.76 | 3.60 |
| $n=1$ | 7.50 | 7.18 | 7.08 | 2.40 | 2.19 | −0.33 | 6.89 | 6.74 | 6.62 | 3.48 |
| | 7.36 | 7.15 | 7.11–7.02 | | | (2.4) | | | | |
| $n=2$ | 7.32 | 7.18 | 7.11–7.02 | 2.43 | | −0.38 | 6.46 | 6.39 | 5.69 | 3.26 |
| | 7.25 | 7.04 | obs | | | (2) | | | | |

[a] $\delta$ Values (ppm from TMS) from $CDCl_3$ solutions at room temperature; obs = obscured.
[b] $^2J$[Rh,H] (Hz) in parentheses.

and only one set of signals for each axial ligand. The $BPh_2$ group gives two sets in the aromatic region (three signals each, the fourth being too broad to be observed), as the phenyls are inequivalent; the shift differences of corresponding carbons are small. Upon introduction of the $BPh_2$ bridge, the adjacent equatorial carbons are deshielded, the other equatorial pairs are slightly shielded; the effects are much stronger for the quaternary than for the methyl carbons. The axial methyl is deshielded by about 3.5 ppm and the L carbon shifts show only small variations.

As pointed out above, **IV** and **V** easily lose a $BPh_2$ bridge in solution; therefore their spectra were recorded in the presence of a two-fold excess of diphenylborinic anhydride. $CH_3Rh(DBPh_2)_2Py$ was obtained in solution by adding a slight excess of Py to a solution of **V**, still in the presence of a two-fold excess of diphenylborinic anhydride. The $^{13}C$ spectra of the bisborylated complexes show one resonance for the equatorial CN, one for the equatorial $CH_3$, one set of resonances for each axial ligand and two sets for the $BPh_2$ groups, being the equatorial phenyls pairwise equivalent; the shift differences of corresponding phenyl carbons are small. The insertion of two $BPh_2$ bridges deshields the axial methyl (about 7 ppm) all the CN carbons and shields all the ring carbons of L. The effects of the stepwise introduction of $BPh_2$ groups are additive for the equatorial carbons and almost additive for the axial methyl.

$^1$H NMR data are reported in Table 4. The excess of diphenylborinic anhydride, added to prevent dissociation, hides some of the signals in the aromatic region. In the $^1$H NMR spectra of both mono- and bisborylated derivatives the axial ligands originate only one set of signals; the phenyls originate two AA'MM'X patterns with well-separated *ortho* proton multiplets, one of these being noticeably deshielded for $CH_3Rh(DH)(DBPh_2)L$ (L = N-MeIm or Py). The equatorial methyls give two resonances in the mono- and one in the bis(diphenylboryl) derivatives; as for the carbons, the effects of the stepwise bridge substitution on the shielding of the equatorial methyl protons are also additive.

As in the cobalt derivatives [5], the first borylation diminishes the shift of the axial methyl protons but, differently from the cobalt derivatives, diminishes, even to a minor extent, those of the pyridine and N-methylimidazole protons. After the second borylation the N-methylimidazole protons are relevantly shielded [2]. The

[2] The *ortho* and *para* protons of Py are hidden by the excess anhydride.

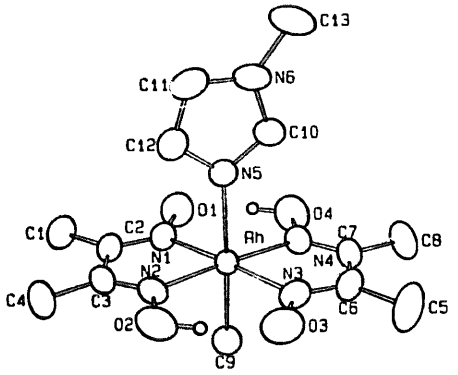


Fig. 7. ORTEP drawing with the numbering scheme for the non-hydrogen atoms of I.

axial methyl is further shielded with L = N–MeIm but deshielded with L = Py with respect to the corresponding monoborylated species.

### 3.4. X-ray structure determinations

ORTEP drawings together with the atom numbering scheme of I and II are shown in Figs. 7 and 8.

The geometry of the $CH_3Rh(DH)_2$ moiety in I is very similar to that found for $CH_3Rh(DH)_2Py$ [9]. In particular, the Rh–N(eq) bonds are two short (mean 1.968(2) Å) and two long (mean 1.981(2) Å), with the corresponding N–O bonds being longer (mean 1.357(3) Å) and shorter (mean 1.331(3) Å) respectively. This allows the location of the oxime bridge H on the O2 and O4 atoms (Fig. 7) to be assigned. The O1 · · · O4 and O2 · · · O3 distances are 2.678(3) and 2.602(3) Å respectively.

A comparison of the axial coordination distances found in I and the $CH_3Rh(DH)_2Py$ analogue [9] shows that the Rh–Me bond length is almost the same in the two complexes (2.060(2) Å in I and 2.063(5) Å in the Py derivative), whereas the Rh–N distance of 2.181(2) Å in I is remarkably shorter than that (2.220(3) Å) found for Rh–Py. This difference may be ascribed to the possibility of a closer approach of N–MeIm to the metal with respect to Py, as already found in the analogous cobaloximes [15].

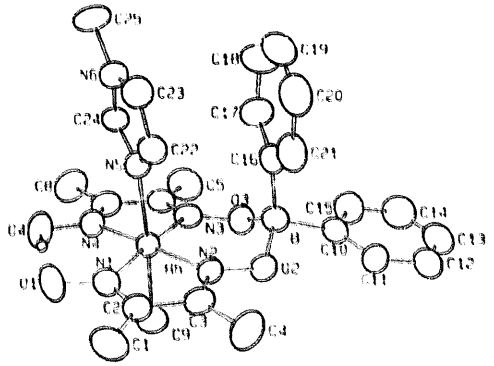

Fig. 8. ORTEP drawing with the numbering scheme for the non-hydrogen atoms of II.

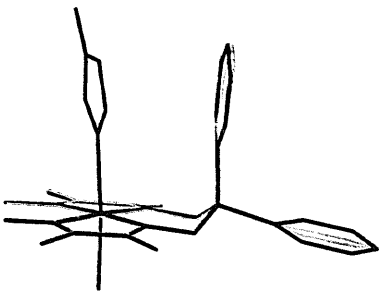

Fig. 9. Scheme of the superimposition of the structures of $CH_3M(DH)(DBPh_2)N$–MeIm with M = Rh and Co. The Rh derivative is represented by the heavy lines.

The geometry of II is characterized by having the axial N–MeIm nearly facing the axial Ph group of the $BPh_2$ bridge (Fig. 8). Their mean planes deviate from the parallel because of a small divergence and a small mutual rotation. The conformation of II is significantly different from that found for the analogous Co complex [5], where the axial Ph group faces the axial Me ligand and the N–MeIm plane is rotated by about 90° with respect to the orientation found in II. The superimposition of the Rh and Co analogues is shown in Fig. 9.

In II the Rh–N(eq) distances exhibit a pattern of three long distances (Rh–N1 1.968(4) Å, Rh–N3 1.978(4) Å, Rh–N4 1.978(4) Å) and one short (Rh–N2 1.940(4) Å), the latter being *trans* to the N4–O4–H grouping (Fig. 8). This pattern has also been observed in the Co analogue. This corresponds to the observation that in rhodoximes the two short Rh–N(eq) distances are those relative to the mutually *trans* N–O–H grouping [16]. Comparison of the O · · · O distance in I and II (Table 5) indicates that a shortening of this distance occurs when an oxime bridge is formally substituted by a $BPh_2$ one. In the Co analogues this substitution does not appear to provoke significant changes in the O · · · O distances. Despite the difference of about 0.1 Å between equatorial Rh–N and Co–N bond lengths, the Rh · · · B

Table 5
Comparison of the axial fragments and O · · · O sites in $CH_3M(DH)_2N$–MeIm and $CH_3M(DH)(DBPh_2)N$–MeIm complexes with M = Co, Rh

| Equatorial moiety | M–C | M–N | O · · · O | |
|---|---|---|---|---|
| C[illegible]$_2$ | 2.009(7) | 2.058(5) | 2.514(8) | |
| | | | 2.483(8) | |
| $Rh(DH)_2$ | 2.060(2) | 2.181(2) | 2.602(3) | |
| | | | 2.678(3) | |
| $Co(DH)(DBPh_2)$ | 1.995(12) | 2.014(9) | 2.469(12) | H |
| | | | 2.510(10) | $BPh_2$ |
| $Rh(DH)(DBPh_2)$ | 2.061(5) | 2.172(4) | 2.729(5) | H |
| | | | 2.577(5) | $BPh_2$ |

(3.208(6) Å) and Co · · · B (3.226(13) Å) distances in **II** and MeCo(DH)(DBPh$_2$)N–MeIm are very similar, as well as the conformations of the six-membered ring including the metal and B atoms. The difference in metal–nitrogen distances is essentially compensated for by small adjustments of some of the internal angles of the cycle, namely an increase of the angles at N (4°) and B (2°) atoms.

Comparison of the axial fragments in CH$_3$M-(DH)$_2$N–MeIm and CH$_3$M(DH)(DBPh$_2$)N–MeIm complexes with M = Co, Rh is summarized in Table 5. The axial bond lengths do not appear to be influenced by the nature of the equatorial ligand. However, the M–N(axial) distance may be significantly influenced by a rotation of the neutral ligand around the M–N(axial) bond. In fact it has been found that when the planar neutral ligand crosses the oxime bridge, the Co–N(axial) bond is shorter with respect to the orientation, differing by a rotation of 90° around this bond [10,16].

## 4. Discussion

It has previously been shown that CH$_3$Co(DH)$_2$L (L = N–MeIm or Py) form stable derivatives containing one diphenylboryl bridge [5]; the present work shows that the Rh complexes have a similar behavior. The results obtained from the present solution studies suggest that both kinetic and thermodynamic effects contribute to their stability. Indeed, the kinetic measurements show that the insertion of the first boron bridge in **I** is about five times faster than that of the second bridge; furthermore, the NMR spectra indicate that **II** does not release the boron bridge in CDCl$_3$ solution. Consequently, CH$_3$Rh(DH)(DBPh$_2$)N–MeIm may be isolated in defect of anhydride. It is likely that the same argument may be applied to explain the stability of CH$_3$Rh(DH)(DBPh$_2$)Py and of the analogous Co complexes.

The stability of the bisborylated complexes compared with the monoborylated ones is lower for the Rh than for the analogous Co derivatives. Indeed, CH$_3$Co(DBPh$_2$)$_2$L (L = N–MeIm and Py) are stable in CDCl$_3$, whereas the corresponding Rh derivatives easily lose one boron bridge in solution and may be isolated only if an excess of anhydride is present. The stability of the bisborylated complexes appears significantly affected by the axial base: CH$_3$Rh(DBPh$_2$)$_2$H$_2$O is stable in solution, but when the steric bulk of the axial base increases an increasing excess of anhydride is necessary to obtain the fully borylated form in solution.

The lower stability of CH$_3$Rh(DBPh$_2$)$_2$N–MeIm in comparison with the analogous Co derivative complexes may be related to the X-ray structural evidence of a remarkable shortening of the O · · · O distance between the oxygens bound by a BPh$_2$ (2.58 Å) and a contemporary lengthening of the O · · · O distance between the oxime oxygens bound by the hydrogen bond (2.73 Å) in **II** relative to the starting rhodoxime (mean value 2.64 Å). It is likely that these structural features may be responsible for the weak association of a second BPh$_2$ group. In the corresponding CH$_3$Co(DH)(DBPh$_2$)N–MeIm complex the insertion of the first BPh$_2$ group causes fewer distortions of the equatorial ligand, with smaller variations in the O · · · O distance [5]. Thus the association of the second BPh$_2$ group is stronger in the cobaloximes with respect to the rhodoximes.

Hence the formation of the bisborylated complexes may be regarded as a stepwise self-assembly process, in which the stability of the final product depends on the distortions induced in the equatorial ring by the introduction of the first boron bridge.

Information on the conformers present in solution may be obtained from the comparison between NMR spectra of the starting bis(dimethylglyoximates) and their borylated derivatives, provided one can distinguish through-space effects from effects due to changes in electronic structure. Indeed, in such complexes the substitution of the hydrogen bridges with BX$_2$ ones affects the electronic structure of the metal. This is reflected by more positive M(III)/M(II) reduction potentials (about 0.6 V for Co [17] and about 0.7 V for Fe [4]) and by different shielding of the cobalt nucleus (about 300 ppm) [17] in the bis(DBF$_2$) relative to the bis(DH) complexes. The strong deshielding of the equatorial C=N and the axial CH$_3$ carbons (Table 3) both in mono- and in bisborylated complexes with respect to the CH$_3$Rh(DH)$_2$L (L = Py, N–MeIm) could be attributed to analogous electronic through-bond effects. However, the strong shielding of the axial ligand protons, especially those four and five bonds apart from the metal center, cannot be explained in the same way and must be due to the ring current of the BPh$_2$ phenyls, as already proposed for the LFe(DBPh$_2$)$_2$L′ systems [4], and supported by comparison between mono- and bisborylated derivatives of cobalt [5]. On this basis a preferred conformation in solution may be indicated for these molecules.

Both for CH$_3$Co(DH)(DBPh$_2$)L [5] and CH$_3$Rh(DH)(DBPh$_2$)L (L = Py, N–MeIm) the preferred orientation in solution has the axial phenyl facing the axial methyl rather than L. This is inferred from the axial methyl protons resonating noticeably upfield, the L protons resonating near those of the parent CH$_3$M(DH)$_2$L compounds, and the BPh$_2$ protons resonating close to those of LFe(DBPh$_2$)$_2$CO (where both the axial phenyls face the axial CO) [4]. The first borylation causes an axial methyl upfield shift slightly smaller in the rhodium than in the corresponding cobalt compound; furthermore, the deshielding of the low field phenyl *ortho* protons is larger in **II** than in its Co analogue [5]. This could indicate that a significant

amount of the conformer with the axial phenyl facing the ligand L is also present in solution of **II**; this suggestion is in agreement with the X-ray structural finding that in **II** the axial phenyl faces the L ligand. A discrepancy between the X-ray structure and the main conformation in solution, as inferred from $^1$H NMR spectra, has been found previously for PyFe(DBPh$_2$)$_2$Py [4] and was attributed to a small difference in energy between the conformers.

In the $CH_3M(DBPh_2)_2L$ compounds (M = Co [5], Rh; L = Py, N–MeIm) the protons of both axial ligands are relevantly shielded (even the $CH_3$ protons of N–MeIm) with respect to those of the starting bis(dimethylglyoximates); therefore both $CH_3$ and L are facing one phenyl, on average. This rules out the strong predominance of a conformer in solution having both the axial phenyls facing the same axial ligand. Furthermore, the pairwise equivalence of four phenyls implies a fast interconformational conversion, as has previously been found in the $LFe(DBPh_2)_2L'$ complexes (L = Py, N–MeIm; L' = CO, $CH_3CN$) [4]. Among the bisborylated complexes, only **IV** shows the axial methyl protons more shielded than in the corresponding monoborylated compound. Perhaps this indicates some excess of the conformer bearing both axial phenyls facing the axial methyl for this complex. However, the X-ray structure of $CH_3Co(DBPh_2)_2CH_3OH$ [5] and the proton chemical shifts of $CH_3M(DBPh_2)_2L$ (M = Rh, Co; L = Py, N–MeIm, $H_2O$) suggest that the main conformation of the equatorial ligand is $C_{2h}$ in all the examined cases, probably because the steric bulk of the axial ligands is not different enough to force the complexes into a $C_{2v}$ conformation.

The conformation adopted by the Fe(II)(DBPh$_2$)$_2$ derivatives having different axial ligands depends essentially on the π–π interactions between the phenyl and the axial ligands, the CH–π interactions playing a minor role [4]. Generally, however, in that case axial ligands with good π-donor or -acceptor properties were used. It has recently been proved that the CH–π properties are able to stabilize the sterically more hindered isomers in some organocobalt and organoaluminium porphyrins [18]. It may be suggested that also for our complexes, all having a methyl as axial ligand, the attractive CH–π interactions may contribute to favor the conformation with the phenyl facing the methyl in the monoborylated complexes and the $C_{2h}$ conformation in the diborylated complexes. Further work is planned to test this hypothesis by using aromatic R groups and boryl bridges containing substituents in the phenyl ring.

## References


[1] B. Köhler, M. Knauer, W. Clegg, M.R.J. Elsegood, B. Golding and J. Rétey, *Angew. Chem., Int. Ed. Engl., 34* (1995) 2389 and references cited therein.

[2] A. Bakac, M.E. Brynildson and J.H. Espenson, *Inorg. Chem., 25* (1986) 4108; K.A. Lance, K.A. Goldsby and D. Busch, *Inorg. Chem., 29* (1990) 4537 and references cited therein.

[3] G.N. Schrauzer, *Chem. Ber., 95* (1962) 1438; F. Umland and D. Thierig, *Angew. Chem., Int. Ed. Engl., 1* (1962) 333; G. Schmid, P. Powell and H. Nöth, *Chem. Ber., 101* (1968) 1205.

[4] D.V. Stynes, D.B. Leznoff and D.G.A. Harshani de Silva, *Inorg. Chem., 32* (1993) 3989; M. Verhage, D.A. Hoogwater, H. vanBekkum and J. Reedijk, *Recl. Trav. Chim. Pays Bas, 101* (1982) 351; D. Stynes, *Inorg. Chem., 33* (1994) 5022; D.G.A. Harshani de Silva, D.B. Leznoff, G. Impey, I. Vernik, Z. Jin and D.V. Stynes, *Inorg. Chem., 34* (1995) 4015.

[5] R. Dreos, G. Tauzher, S. Vuano, F. Asaro, G. Pellizer, G. Nardin, L. Randaccio and S. Geremia, *J. Organomet. Chem., 505* (1995) 135.

[6] Unpublished results of these laboratories.

[7] B. Giese, J. Hartung, C. Kesselheim, H.J. Lindner and J. Svoboda, *Chem. Ber., 126* (1993) 1193.

[8] R. Dreos Garlatti, G. Tauzher, M. Blaschich and G. Costa, *Inorg. Chim. Acta, 105* (1985) 129; R. Dreos Garlatti, G. Tauzher and G. Costa, *Inorg. Chim. Acta, 121* (1986) 27; S. Geremia, L. Randaccio, R. Dreos and G. Tauzher, *Gazz. Chim. Ital., 125* (1995) 95.

[9] N. Bresciani Pahor, R. Dreos Garlatti, S. Geremia, L. Randaccio, G. Tauzher and E. Zangrando, *Inorg. Chem., 29* (1990) 3437.

[10] L. Randaccio, S. Geremia, R. Dreos Garlatti, G. Tauzher, F. Asaro and G. Pellizer, *Inorg. Chim. Acta, 194* (1992) 1.

[11] J.H. Espenson and R.C. McHatton, *Inorg Chem., 20* (1981) 3090; R. Dreos Garlatti and G. Tauzher, *Polyhedron, 9* (1990) 2047.

[12] J. Emri and B. Györi, in G. Wilkinson (ed.), *Comprehensive Coordination Chemistry*, Vol. 3, Pergamon Press, Oxford, 1987, p. 81 and references cited therein.

[13] W.H. Zachariasen, *Acta Crystallogr., 16* (1963) 1139.

[14] *MolEN, An Interactive Structure Solution Procedure*, Enraf–Nonius, Delft, Netherlands, 1990.

[15] N. Bresciani-Pahor, S. Geremia, C. Lopez, L. Randaccio and E. Zangrando, *Inorg. Chem., 29* (1990) 1043.

[16] N. Bresciani-Pahor, W.M. Attia, S. Geremia, L. Randaccio and C. Lopez, *Acta Crystallogr., C45* (1990) 561.

[17] C. Tavagnacco, G. Balducci, G. Costa, K. Täschler and W. von Philipsborn, *Helv. Chim. Acta, 73* (1990) 1469.

[18] H. Sugimoto, T. Azida and S. Inoue, *J. Chem. Soc., Chem. Commun.*, (1995) 1411.